Polymer 51 (2010) 4726–4734

Contents lists available at ScienceDirect

Polymer

journal homepage: www.elsevier.com/locate/polymer

Online monitoring of the copolymerization of 2-(dimethylamino)ethyl acrylate with styrene by RAFT. Deviations from reaction control

Zheng Li [a], Algirdas K. Serelis [b], Wayne F. Reed [a], Alina M. Alb [a,*]

[a] Dept. of Physics and Tulane Center for Polymer Reaction Monitoring and Characterization (PolyRMC), Tulane University, New Orleans, LA 70118, USA
[b] DuluxGroup, 1956 Princes Highway, Clayton, Victoria 3168, Australia

ARTICLE INFO

Article history:
Received 25 June 2010
Received in revised form
4 August 2010
Accepted 6 August 2010
Available online 14 August 2010

Keywords:
RAFT polymerization
Light scattering
Degradation

ABSTRACT

Kinetics of copolymerization reactions of 2-(dimethylamino)ethyl acrylate (DMAEA) and styrene by reversible addition fragmentation transfer (RAFT) in *N,N*-dimethylformamide (DMF) are reported. Novel approaches in the online monitoring of the synthesis of the amphiphilic copolymers by Automatic Continuous Online Monitoring of Polymerization reactions (ACOMP) are presented. Automatic withdrawal of separate reactor streams and their subsequent dilution throughout the reaction with organic and aqueous solvents, respectively, allowed different features to be captured. Thus, light scattering data combined with spectroscopic and viscometric measurements in DMF, together with conductivity measurements in aqueous medium provided in real time comonomer conversion, copolymer mass, reduced viscosity, and composition. Continuous data gathered allowed observing and quantifying the DMAEA-linked macroRAFT control agent decomposition, with significant effects on the reaction kinetics. Deviations from controlled behavior were investigated during (co)polymerization reactions under different conditions.

Multi-detector Size Exclusion Chromatography (SEC) and NMR were used to bring additional information on the system investigated.

Published by Elsevier Ltd.

1. Introduction

Free radical polymerization has been revolutionized in recent years by the introduction of controlled (CRP) techniques [1], which confer control over the polymerization process while maintaining the versatility of conventional free radical polymerization. Synthesis of block, gradient or other polymers of complex architecture, with predetermined molecular weight, narrow molecular weight distribution, and high degrees of chain end functionalization is no longer a difficult challenge [2–8].

Among CRP methods, much attention has been devoted to reversible addition fragmentation chain transfer (RAFT) as a versatile method that allows different materials with well defined molecular structures and architectures to be obtained [9–16]. While this approach proved to be an efficient and attractive means for a wide range of monomers and reaction conditions, side reactions and deviations from ideality due to incompatibility between certain monomer types and control agents, and experimental conditions are reported [4,17,18].

Despite some controversy in terminology [19], usually, the level of control is assessed based on the narrowness of the molecular weight distribution (MWD) and on the linear increase of the number-average molecular weight, M_n with conversion, whereas the livingness is quantified in the fraction of dormant polymer chains that can be extended by the addition of new monomer.

Automatic Continuous Online Monitoring of Polymerization reactions (ACOMP) [20–22] joins other techniques which study and quantify RAFT polymerization kinetics under different conditions [23–27]. Recently, the authors reported the online determination of MWD by coupling for the first time automated multi-detector SEC with the continuous non-chromatographic based ACOMP method to obtaining M_w [28]. The online chromatographic addition is particularly useful in the case of the controlled reactions, with slow kinetics where detailed knowledge of the MWD is required. Chain extension and end group analysis are among the methods used to asses reaction livingness, i.e. the number fraction of dormant polymer chains [29].

ACOMP was used here to follow in real time the synthesis of 2-(dimethylamino)ethyl acrylate (DMAEA)/styrene copolymers by RAFT. The goal of this work is twofold: first, to study the feasibility of a new approach in studying the synthesis of amphiphilic copolymers by simultaneous online measurements in different

* Corresponding author. Tel.: +1 504 862 3186.
E-mail address: aalb@tulane.edu (A.M. Alb).

0032-3861/$ – see front matter Published by Elsevier Ltd.
doi:10.1016/j.polymer.2010.08.015

solvents, and second to investigate the degradation process of the macroRAFT control agent during the copolymerization reactions, presumably caused by the tertiary amine group of DMAEA.

Poly[2-(dimethylamino)ethyl acrylate], poly(DMAEA) is a pH-sensitive polymer in aqueous solution, as its tertiary amine can be quaternized at low pH, with wide applications in the pharmaceutical and water treatment industries [30]. However, polymerization of DMAEA by RAFT means is less studied [31–33], due to the challenges imposed by the low steric hindrance of its substituents and side reactions of the polar amino group [34].

2. Experimental

2.1. Materials

Styrene (Sty, ≥ 99%, *ReagentPlus*®), DMAEA (98%) *2,2′*-azoisobutronitrile (AIBN, 98%) *N,N*-dimethylformamide, (DMF, ≥99.8%, A.C.S. grade), anhydrous DMF (99.8%), tetrahydrofuran (THF, ≥ 99.9%, anhydrous), dioxane (99.8%, anhydrous), toluene (99.8%, anhydrous), and n-butyl acrylate (BA, 99+ %), were used as received from Aldrich. The main trithiocarbonate (TTC) used as RAFT control agent, 2-{[(dodecylsulfanyl)carbonothioyl]sulfanyl}propanoic acid (DoPAT) and the dimethylaminoethyl ester of DoPAT were provided by DuluxGroup. DoPAT structure is shown in Scheme 1. Dibenzyl trithiocarbonate (DBTTC) from Arkema, France, and 4-cyano-4-(ethylsulfanlthiocarbonyl)sulfanylpentanoic acid (CEP) [35] were also used. Trithiocarbonates are used in many applications, with a generally good kinetic behavior combined with superior resistance to hydrolysis [36] in aqueous media [6–11,37].

The polymerization reactions were carried out with a total of ~30% by mass of monomer in DMF at 80 °C in a 150 ml three-neck round bottom flask reactor equipped with a condenser, under magnetic stirring. The initial volume of reactor fluid was 100 mL. Nitrogen flow was applied before and maintained throughout the reactions.

2.2. Techniques

A recent ACOMP methodology [38] consisting of automatic and continuous withdrawal and dilution of the reactor solution with different solvents was adapted in this work in order to simultaneously measure different properties. Thus, a first small stream withdrawn from the reactor was diluted in two stages with DMF and passed through detectors comprising a Brookhaven Instruments Corporation (BI-MwA) multi-angle light scattering detector, a Shimadzu differential refractometer (RID-10A), a custom-built single capillary viscometer [39], and a Shimadzu photodiode array UV/visible spectrophotometer (SPM-20A) that covers the 200–800 nm spectral range. This set-up allowed online monitoring of conversion, comonomer composition, copolymer mass, and reduced viscosity to be determined. The diluted reactor solution (~2.3 mg/ml) was passed through detectors at 2 ml/min during the reaction and data were collected every 2 s, with an 8 min lag time between reactor extraction and detector measurements. On the other hand, dilution with aqueous solvent of a second stream taken from the reactor allowed in-situ conductivity measurements to be made and the consumption of the amine-containing monomer to be followed, the results being used in the copolymer characterization. In this case, the dilution in a low pressure mixing chamber was about 20×.

Multi-detector SEC was carried out offline using the ACOMP detector train, to which two chromatographic columns, PL gel 5 μ, 50 Å, 300 × 7.5 mm and PL gel 5 μ, 500 Å, 300 × 7.5 mm, connected in series and an injector with a 0.1 ml loop were added. The eluting solvent, DMF (≥99.8%, A.C.S. grade, used as received and replaced each 24 h) was passed through detectors and columns at 0.6 ml/min. SEC was used to determine MWD and dispersity, and to cross check ACOMP results on conversion and molecular weight.

^{13}C NMR measurements were conducted on a Bruker Avance 300 NMR Spectrometer with the frequency of 75 MHz, using $CDCl_3$ as solvent.

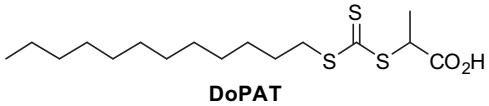

Scheme 1. DoPAT structure.

3. Results and discussion

Table 1 gives a summary of the copolymers synthesized, along with experimentally determined characteristics from ACOMP continuous measurements. The $(dn/dc)_p$ values listed in the table are determined for each copolymer in separate experiments made with the endproducts of the ACOMP monitored reactions. An example of these experiments and a short description of the method are given in Supporting Information (Fig. S8, Supp. Inf). It is important to mention here that *dn/dc* for a copolymer changes during the reaction, as function of composition and chain length and could affect M_w determination. A workable and practical formalism was reported in a previous work [40] for determination of M_w during reaction, using a single solvent, developed for the case of *N* comonomers. However, in this work, it is believed that the effect of the above mentioned factors is minimal, based on the agreement between two independent method used to determine concentrations (Fig. 2): from SEC, by quantifying the decrease in the comonomer absorbance peaks (no constants used, just integrating the UV peaks) and from ACOMP using the UV&RI data with *dn/dc* and extinction coefficients ε independently measured for the endproducts of the reactions monitored.

3.1. Raw data

Data gathered from the multiple detectors of ACOMP are used in different parts of analysis and furnish important information on the process monitored.

Fig. 1a shows raw data for reaction A3 (10/90 Sty/DMAEA) from ACOMP multi-detector train. Typically, after the solvent baseline

Table 1
List of experiments and their conditions. ACOMP results: reaction rate constant, κ, weight-average molecular weight, M_w (based on light scattering data) at the final monomer conversion, ρ, reduced viscosity, η_h, and *dn/dc* values for each endproduct are listed.

#	[Sty]/[DMAEA]	κ (s^{-1})	$M_{w@\rho}$ (g/mole)	$\eta_{r@\rho}$ (cm^3/g)	ρ	$(dn/dc)_p$
A1	2/98	2.378×10^{-4}	21800	10.4	0.76	0.042
A2	5/95	1.543×10^{-4}	25000	8.6	0.69	0.047
A3	10/90	1.057×10^{-4}	26600	7.8	0.59	0.059
A4	20/80	6.161×10^{-5}	28300	8.6	0.59	0.063
A5	30/70	7.696×10^{-5}	32200	8.2	0.57	0.067
A6	50/50	8.716×10^{-5}	30600	10.7	0.49	0.080
A7	0/100	2.204×10^{-4}	15500	7.1	0.67	0.047
A7b[a]	0/100	NA	NA	NA	NA	NA
A8	100/0	NA	NA	NA	0.19	0.111
B1[b]	0/100	6.716×10^{-4}	31000	16.2	0.79	
B2[b]	10/90	7.081×10^{-5}	28900	16.0	0.68	0.031

All the experiments were made at 80 °C in DMF under N_2 flow. Total monomer concentration was 2.5 M, [DoPAT]/[AIBN] = 2, [M]/[DoPAT] = 360.
[a] Reaction in batch; [M]/[DoPAT] = 10.
[b] DMAEA was replaced by BA.

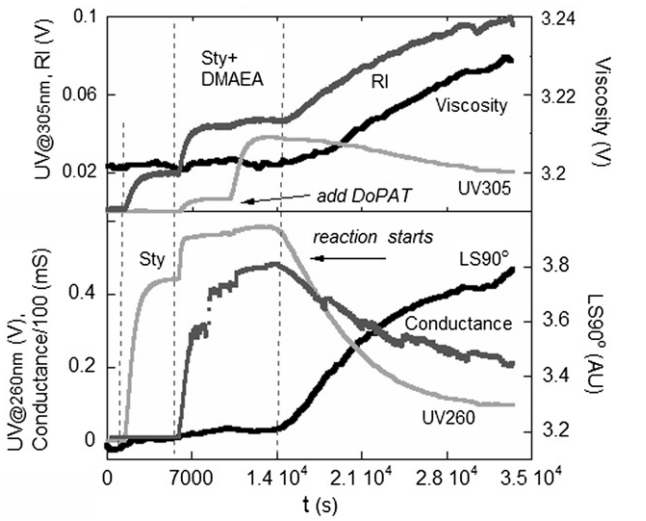

Fig. 1a. Raw data for Sty/DMAEA (10/90) copolymerization (A3, listed in Table 1).

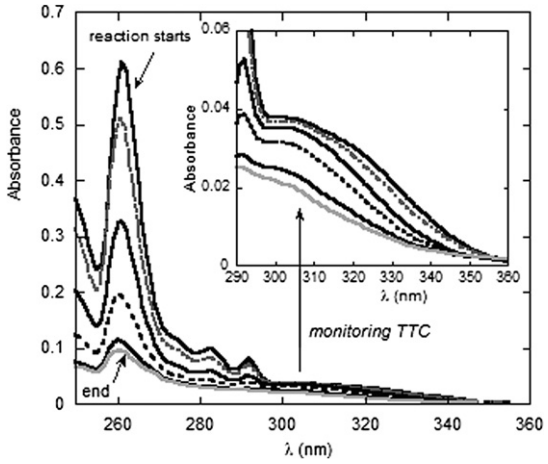

Fig. 1b. Selected UV absorbance spectra during the copolymerization for reaction A3.

was stabilized, continuous withdrawal/dilution of the reactor content started and allowed comonomers and DoPAT baselines to be obtained. As the temperature reached the preset value (80 °C), AIBN was added (~14000 s) and the reaction started.

As shown in the figure, the decrease in the UV absorbance (at 260 nm) and in conductivity signals follows the monomer consumption whereas the steady increase in RI, viscosity and LS data throughout the reaction indicates the polymer production. The fact that UV absorbance is continuously recorded over a broad spectral range allows not only the consumption of the monomer to be followed but also other types of reactions. Thus, UV absorbance at 305 nm, shown also in Fig. 1a, was used to monitor the concentration of the TTC moiety during its transfer from DoPAT to the initial macroRAFT species, and subsequent polymer growth from the latter. The monitoring of this signal during the reaction allows an important process to be detected and followed, decomposition of the TTC, a reaction found to occur simultaneously with the polymerization, with crucial impacts on reaction control. No degradation occurred before the addition of the initiator, as shown by the constant UV signal at 305 nm while the comonomer/DoPAT mixture was kept at 80 °C.

Fig. 1b gives examples of UV absorption spectra from 250 nm to 360 nm at selected times. Full spectra were collected every 2 s.

3.2. Comonomer concentrations and conversion

Continuously collected RI and UV signals from ACOMP were used to calculate comonomer concentrations. As a novel feature, an alternate route to follow DMAEA concentration was provided in this work by the use of the online monitored conductivity of this monomer in aqueous medium, based on the change in the signal due to incorporation of the monomer into the less electrophoretically mobile copolymer chains.

Both comonomers, the copolymer produced during reaction, and the RAFT control agent were taken into account in the calculations under the assumption that the signals from UV and RI are simply the sum of the relative signals from each species. Thus,

$$V_{RI} = \left[\left(\frac{dn}{dc}\right)_A c_A + \left(\frac{dn}{dc}\right)_B c_B + \left(\frac{dn}{dc}\right)_P c_P + \left(\frac{dn}{dc}\right)_D c_D\right] \Big/ CF \qquad (1)$$

$$V_{UV} = (\varepsilon_A c_A + \varepsilon_B c_B + \varepsilon_P c_P + \varepsilon_D c_D)\cdot l \qquad (2)$$

where CF is a calibration factor for RI, l the path length of the UV cell, dn/dc and ε are the incremental refractive index value and UV extinction coefficients, respectively, determined from the reactions. In all formulae, $c_{A\,(B)}$ refers to the mass concentration of species A (B), c_p and c_D are the mass concentrations of the polymer and of DoPAT, respectively.

The equations above together with the mass conservation equation,

$$c_P = c_0 - c_A - c_B \qquad (3)$$

where c_0 is the total initial concentration of the monomers, allow the comonomer concentrations to be computed:

$$c_B = \frac{(\varepsilon_A l - \varepsilon_P l)[V_{RI} CF - (\frac{dn}{dc})_D c_D - \left(\frac{dn}{dc}\right)_P c_0] - \left[\left(\frac{dn}{dc}\right)_A - \left(\frac{dn}{dc}\right)_P\right](V_{UV} - \varepsilon_D l c_D - \varepsilon_P l c_0)}{(\varepsilon_P l - \varepsilon_B l)\left[\left(\frac{dn}{dc}\right)_A - \left(\frac{dn}{dc}\right)_P\right] - (\varepsilon_A l - \varepsilon_P l)\left[\left(\frac{dn}{dc}\right)_P - \left(\frac{dn}{dc}\right)_B\right]} \qquad (4)$$

$$c_A = \frac{V_{UV} - \varepsilon_D l c_D - \varepsilon_B l c_B - \varepsilon_P l (c_0 - c_B)}{\varepsilon_A l - \varepsilon_P l} = \frac{V_{RI} CF - \left(\frac{dn}{dc}\right)_D c_D - \left(\frac{dn}{dc}\right)_B c_B - \left(\frac{dn}{dc}\right)_P (c_0 - c_B)}{\frac{dn}{dc_A} - \frac{dn}{dc_P}} \qquad (5)$$

The computed incremental refractive index, dn/dc values, for the comonomers and copolymers are given in Tables 1 and 2.

As mentioned, the ACOMP multi-detection gives flexibility in choosing the most appropriate method to compute the comonomer concentrations during a reaction. The addition of the conductivity probe gave an alternate means of assessing DMAEA concentration

Table 2
Computed *dn/dc* values for the comonomers and the RAFT control agent in DMF. These are averaged over the dn/dc values determined during each reaction based on the RI data gathered during each of the reactor component baseline.

DMAEA	Styrene	BA	DoPAT
0.0097 ± 0.8%	0.106 ± 5.3%	−0.0089	0.118 ± 1.0%

on an empirical basis, as it is weakly charged in water, to a small but sufficient extent for conductivity measurements to be made. When DMAEA is polymerized into a chain, the conductivity decreases [41], since the electrophoretic mobility of the chain per monomer is less than that of the free monomer. Without any assumptions about the chain electrophoretic mobility vs. that of free DMAEA, the first-order rate constant that is obtained from the fit to the conductivity data is virtually identical to that obtained via the UV/RI method, demonstrating that the conductivity changes are due entirely to the DMAEA conversion. If the final plateau value of conductivity is taken as full conversion then DMAEA concentration can be obtained by

$$c(\mathrm{t}) = \frac{\delta(\mathrm{t}) - \delta_\mathrm{f}}{\delta(0)} c_0 \tag{6}$$

where $\delta(\mathrm{t})$ is the conductivity at time t, $\delta(0)$ is the conductivity of the solution due to DMAEA before the reaction has started, and δ_f is the measured final value.

An example of the complementarity of the possible approaches is shown in Fig. 2 for reaction A3. A schematic representation of the dilution process in ACOMP front-end is also shown. Thus, the fact that c_{DMAEA} from the method based on spectroscopic detection (eqs. 4 and 5) is in agreement with the data furnished by the monitored conductivity signal (eq. (6)) proves the feasibility of the latter approach in following the concentration of the charged monomer. Additionally, concentration values from SEC on manually withdrawn aliquots, shown as discrete points in the figure are in excellent agreement with the ACOMP values.

The computed concentrations from either one of the methods described above allowed the total comonomer conversion ρ to be determined, shown in Fig. 3 for selected experiments. First-order function fits are applied to conversion data:

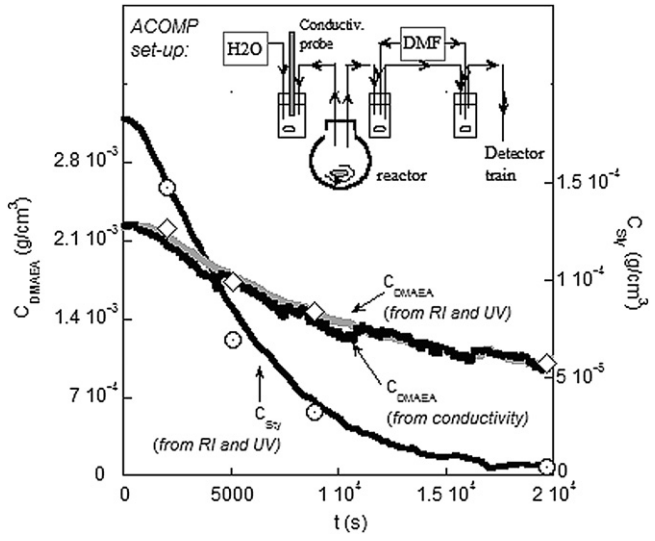

Fig. 2. Comonomer concentrations as functions of time based on RI, UV and conductivity data for the reaction A3 in Table 1. The discrete points are the concentration values by SEC experiments on manually withdrawn aliquots.

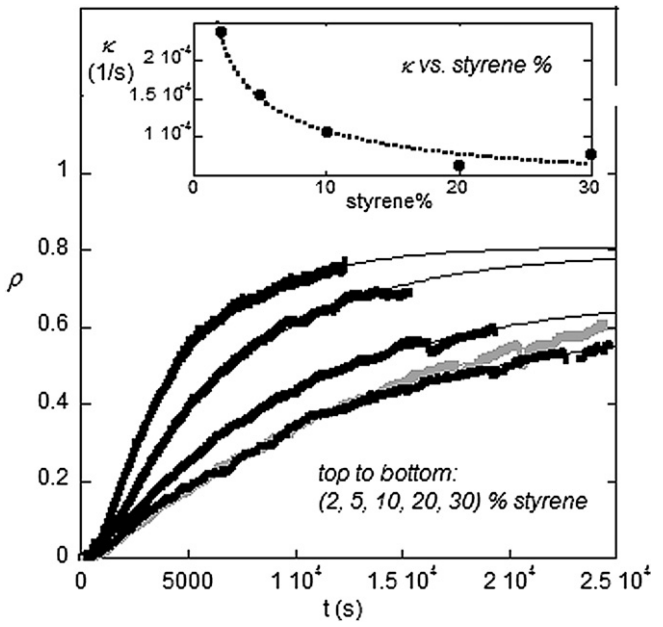

Fig. 3. Total monomer conversion ρ with first-order function fits for the A1−A5 copolymerization reactions listed in Table 1. In the inset to figure, the reaction rate coefficient, κ vs. styrene% in the initial composition.

$$\rho = 1 - e^{-\kappa t} \tag{7}$$

where ρ is the total conversion (based on the concentrations in molar units).

As shown in the inset to the figure, κ increases as the amount of styrene decreases in the initial composition.

3.3. Composition drift

The ACOMP continuously collected data eliminate the use of discrete measurements or traditional model-dependent methods, rather provide information in real time on copolymer composition, experimentally determined at each moment during the reaction. The instantaneous composition drift of a comonomer A, $F_{\mathrm{inst,A}}$ is computed from the comonomer concentrations, using

$$F_{\mathrm{inst,A}} = \frac{d[\mathrm{A}]/dt}{d[\mathrm{A}]/dt + d[\mathrm{B}]/dt} \tag{8}$$

Thus, Fig. 4 shows the online data for the instantaneous styrene composition drift, $F_{\mathrm{inst,sty}}$ for a series of Sty/DMAEA copolymerization reactions with different initial composition, A2-A6. The highest composition drift occurs for Sty/DMAEA 10/90 reaction. The azeotrope, for which $F_{\mathrm{inst,sty}}$ is constant should be near Sty/DMAEA 20/80. The trends in composition drift curves are similar to those reported in the case of nitroxide mediated copolymerization of styrene with acrylates [42].

The continuous F_{inst} data provided by ACOMP allows assessment of the effect of the rate of styrene incorporation in the copolymer on the evolution of the main CRP features during the copolymerization.

It is important to point out that obtaining that one of the ACOMP advantages is the model-independent determination of the comonomer concentrations and hence of the composition drift/distribution as the reaction occurs. The notion of reactivity ratios and the various formulations to express them, in contrast, are model-dependent. In some sense, ACOMP makes unnecessary the

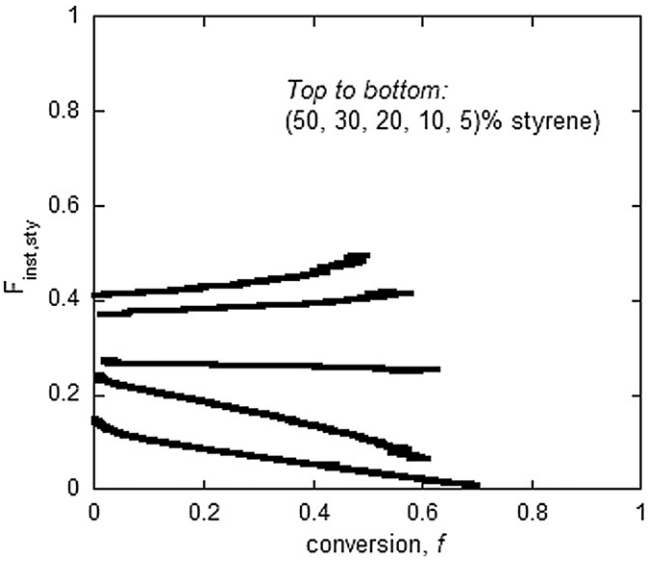

Fig. 4. Styrene instantaneous composition drift, $F_{inst,Sty}$ for the Sty/DMAEA copolymerization reactions A2, A3, A4 and A6, in Table 1.

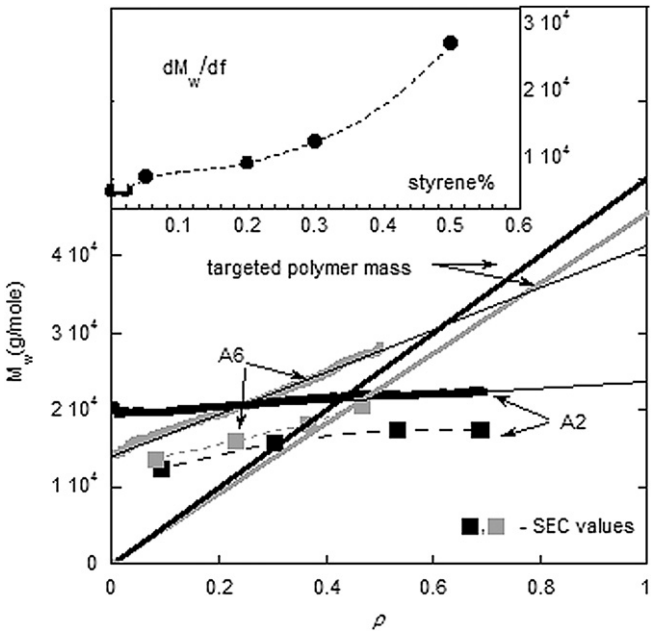

Fig. 5. M_w vs. conversion for two copolymerization reactions with different initial composition, A2 and A6, in Table 1. Discrete points represent SEC data.

use of reactivity ratios because it yields the average composition distribution as it evolves during the reaction and automatically detects any unexpected or nonideal effects that may occur in a reaction, but which are not normally predicted by idealized models. Nonetheless, the reactivity ratios are still important for their predictive power, their practical use in helping to optimize reactions, their inherent theoretical interest, and for historical reasons.

Data on reactivity ratios are not reported here due to the fact that it was found they depend on the model used (terminal vs. penultimate effects) and more investigation is ongoing.

3.4. Molecular weight and MWD

The computed comonomer concentrations are used in the determination of M_w together with data from the absolute light scattering measurements, based on Zimm equation [43]. Recent work established the formalism for determining M_w for copolymers, based on the multi-angle light scattering data [40].

It is important to point out the unique advantage ACOMP offers by providing continuously collected data that allows more detailed information about reaction kinetics to be obtained, features not easily observed with the limited number of measurements from discrete methods. Thus, deviations from linearity in the M_w vs. ρ typical CRP plots that indicate loss of control, branching, etc could be easily missed if only discrete M_w values were used.

The evolution of M_w with conversion for two copolymerization reactions with different initial composition, A2 and A6 is shown in Fig. 5. The inset to the figure shows dM_w/df vs. % of styrene in the initial monomer composition. As the initial amount of styrene increases, the reaction control is more pronounced, seen in the increase in dM_w/df values. Better control is observed in the case of A6 reaction, with higher amount of styrene, illustrated by the M_w increase in controlled fashion and reach of the target mass. As seen in the figure, although both linear, M_w for A2 has almost zero slope, indicating the polymerization is effectively uncontrolled, whereas the higher slope of M_w for A6, closer to the target value, is more 'living-like'. However, all the reactions show high M_w intercept at $\rho = 0$, indicating a hybrid behavior at low conversion, which is commonly reported [44–46]. Because the transfer rate coefficient for the transfer reactions, k_{tr}, during the RAFT pre-equilibrium is too low compared to the propagation rate coefficient, k_p [47], some of the CTA molecules are only slowly converted into polymer chains, thus resulting in the existence of chains formed from both conventional free radical as well as RAFT polymerization mechanism. Additionally, as discussed in the next section, in the case of DMAEA, side reactions and abnormally high levels of termination occur and lead to a decrease in the fraction of living chains (L).

In this work, M_w was determined during each reaction based on the light scattering data provided by the ACOMP continuous measurements and SEC measurements were used mainly for cross checks on comonomer conversion and for information on dispersity. Unfortunately, in the context of SEC, the small molecular weight targeted, low polymer concentration, together with the small dn/dc values of the polymer in DMF made not possible the use of light scattering in the analysis. The lack of the viscosity signal did not allow the use of a universal calibration curve, which would account for hydrodynamic volume difference. Therefore, polymer mass in the SEC context was determined, based on the calibration with polystyrene standards. Results from this method, shown often to be less accurate and potentially misleading [48,49] are lower than the absolute values from ACOMP, listed in Table 1 (M_w). For better visualization of this discrepancy and emphasis of the usefulness of light scattering detection, a comparison between M_w values from SEC and ACOMP is made in Fig. 5. Listed in Table 3 are M_n, M_w, and M_z, together with dispersity indices obtained by SEC using calibration with polystyrene standards, ($M = 6.4046 \times 10^{10} + 10\times$ (elution volume)$^{-6.0565}$, polystyrene mass range: 1600–30000 g/mol) along with the target mass values [48] for the respective reactions. For better comparison, results from measurements made at similar conversion ($\rho_{\equiv}$) are listed.

3.5. Side reactions. Loss of control due to the DMAEA-linked macroRAFT control agent degradation

Both the continuously monitored UV data from ACOMP (Figs. 1,7 and 8) and the discrete raw RI and UV data from SEC chromatograms of samples withdrawn during the reactions studied (Figs. 9 and 10, experiment #A2) indicate a degradation of the

Table 3
SEC results: M_w, M_n, M_z and M_w/M_n values for the copolymer endproducts of the reactions listed in Table 1.

#	$M_{n@f\equiv}$ (g/mole)	$M_{w@f\equiv}$ (g/mole)	$M_{z@f\equiv}$ (g/mole)	M_w/M_n	M_z/M_w	$\rho_{\equiv}$ [a]	$M_{n,th@\rho\equiv}$ [b] (g/mole)
A1	9300	12700	17500	1.36	1.38	0.42	21800
A2	12800	17400	21100	1.36	1.21	0.53	27200
A3	14000	18800	23000	1.34	1.22	0.45	22900
A4	15100	19100	22900	1.26	1.20	0.47	23200
A5	16000	19500	22700	1.21	1.16	0.49	23500
A6	16700	20600	22700	1.24	1.10	0.49	22100
A7	9000	12200	15100	1.35	1.24	0.55	9000

[a] $\rho_{\equiv}$ is the conversion at which the SEC measurements were made.
[b] $M_{n,th,@\rho}$ is calculated according to literature [48].

trithiocarbonate group presumably caused by the amine group of DMAEA, a process that has a negative effect on the controlled character of the polymerization. DMAEA polymerization reaction was reported by other groups [32,34] but as the authors are aware, this is first time when the TTC degradation is observed, within the condition studied. One possible explanation could be the lack of continuous data provided by thee online monitoring. Thus, in the case of M_w as function of conversion, numerous publications report controlled behavior based on discrete measurements and on a linear extrapolation of these points. Deviations from control, branching, chain transfer phenomena, at different stages of the reaction might be missed.

Therefore, the study focused next on the behavior of the TTC as different factors such as monomer concentration, monomer type, solvent, addition of a second monomer were varied.

Two ways that the amine group of DMAEA could lead to the TTC degradation were thought, either (1) acting as a nucleophile to directly attack the C═S and catalyze cleavage of the TTC, or (2) acting as a base to remove the proton on the terminal carbon between the ester carbonyl and the TTC to trigger an eliminative fragmentation of the TTC.

NMR measurements were made on samples during a DMAEA polymerization reaction (A7b) with a high amount of DoPAT so that

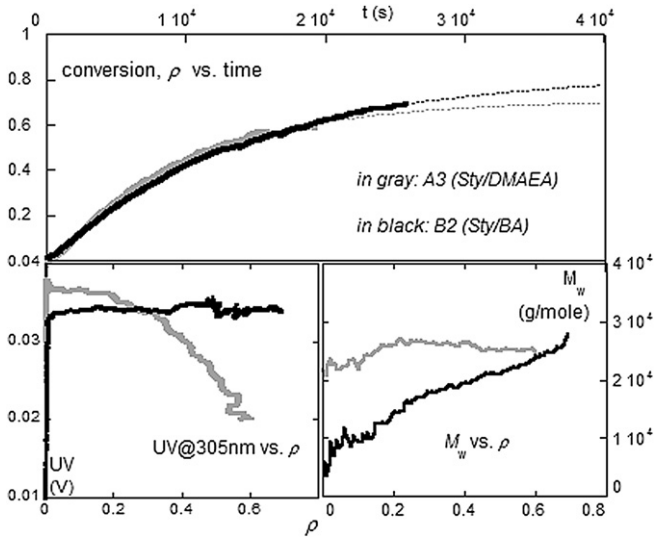

Fig. 7. *Above*: total monomer conversion ρ during A3 and B2 reactions, Table 1. *Below:* UV absorbance @305 nm vs. time (left) and M_w vs. ρ for the same reactions (right).

different signatures would be easier to identify ([DMAEA]/[DoPAT] = 10). Fig. 6 shows ^{13}C NMR results from the reaction A7b from samples taken before the reaction had started (A) and 5 h after the initiator was added (B). The decrease in intensity of peak *2* and *3* indicates the monomer polymerizes, since the peaks belong to the monomer C═C bonds. Most of the signals in DoPAT are still present but shifted more or less and somewhat broadened due to its consumption and incorporation into the polymer. The carboxylic acid group at ~175.7 ppm (peak *8*) had shifted to ~174.4 ppm as it attached to the polymer chains. However, data indicate the thiocarbonyl carbon (peak *7*) has disappeared. Based on the NMR data, it can be concluded that DoPAT has been almost completely consumed, the R-group still exists, presumably attached to the

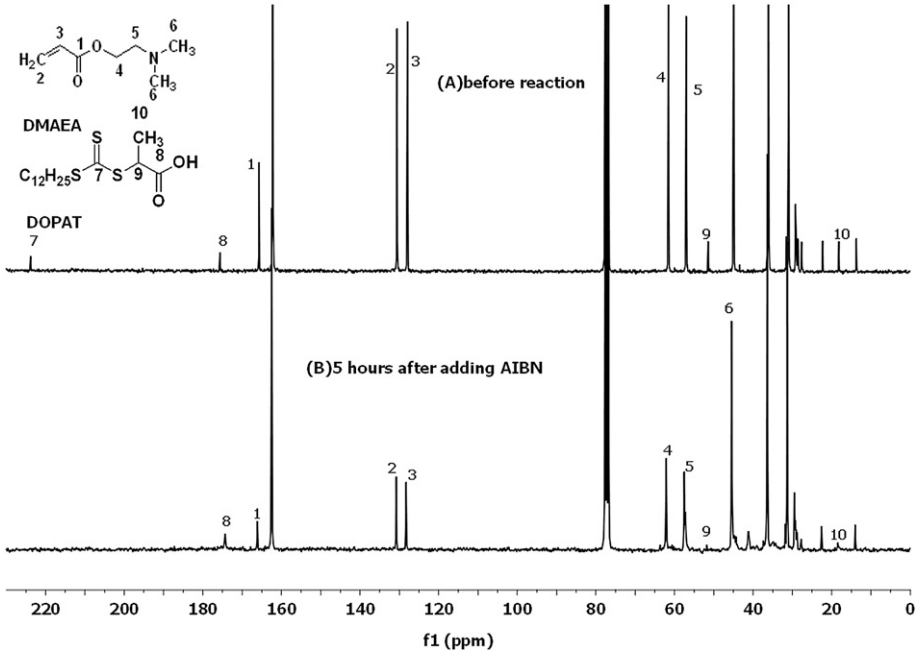

Fig. 6. NMR data for A7b, DMAEA polymerization reaction ([M]/[DoPAT] = 10).

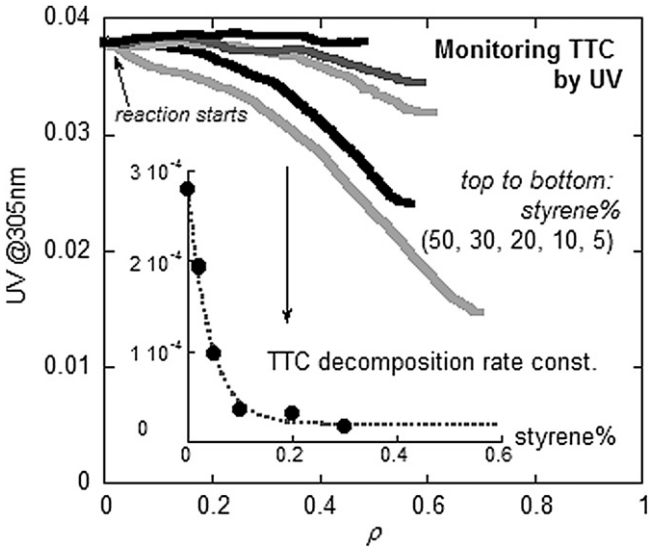

Fig. 8. UV absorbance @305 nm vs. conversion from ACOMP for reactions in Table 1.

polymer, but the trithiocarbonate group S–C(=S)–S has been destroyed. The conclusion that the trithiocarbonate was degraded is based not only on the disappearance of the thiocarbonyl carbon (peak 7) observed by NMR but also on the corroborated results from ACOMP – UV305 decrease throughout the reaction and SEC – UV305 evolution vs. elution volume. A better visualization of the facts explained in the case of experiment A7b is offered in Fig. S1 in the Supporting Information, which is a zoom in on the Fig. 6.

3.5.1. Solvent effect

A first step in assessing the factors affecting the behavior of the TTC moiety in the polymerization of DMAEA was to eliminate the effect of other species, such as inhibitors, water on the reaction kinetics. However, the results from DMAEA polymerization reactions performed with the purified monomer, at different concentrations, in anhydrous DMF indicate that the degradation of the TTC still occurs. Additional experiments in which DMF was replaced by other solvents such BA, THF, dioxane and toluene led to same results, i.e TTC moiety being degraded during the polymerization. Results of these experiments are included in the Supporting Information, section 2. TTC degradation in THF was previously reported [50].

3.5.2. Monomer effect

A first attempt to improve the reaction control during DMAEA polymerization was related to its tertiary amine group. Thus, methyl iodide was used to quaternize DMAEA, subsequently polymerized under the same conditions. It was found that the use of the trimethylammonium analogue of DMAEA does not eliminate the TTC degradation.

Next, to confirm that the decomposition of the TTC moiety is due to the amine group of DMAEA, DMAEA was replaced with butyl acrylate (BA) in two reactions, B1 and B2, listed in Table 1. For comparison purposes, Fig. 7 shows the total conversion for reactions A3 and B2, copolymerization reactions of DMAEA with styrene and BA, respectively. Whereas reaction rates are not significantly different, and the conversion curves strongly overlap, a totally different situation is observed in the TTC behavior, illustrated in the evolution of UV data at 305 nm for the two reactions.

The UV signal is constant during the copolymerization of styrene with BA, indicating that no decomposition of the TTC occurs in this case, as opposed to the strong UV loss in the case of the DMAEA copolymerization reactions. Therefore, as expected, the BA/Sty copolymerization exhibits very good controlled behavior, denoted by the linear increase of M_w with conversion and narrow MWD. The monomer is being consumed at the same rate and the kinetics are similar in a first-order approximation. However, the difference in molecular weight evolution comes from the loss of control occurring in the case of the Sty/DMAEA copolymerization reaction. Termination and side reactions favored by the degradation of the TTC affect the M_w behavior.

3.5.3. RAFT control agent effect

Next, the effect of the chosen RAFT control agent was considered. DoPAT was replaced with a different TTC, in order to test whether the carboxylic acid in DoPAT played any role in the observed decomposition, triggered by the amine group of DMAEA. DBTTC and CEP were used in DMAEA polymerization reactions and led to similar effects as in the cases where DoPAT was used; i.e. the same strong loss of UV signal at 305 nm was observed, indicating TTC degradation.

3.5.4. Comonomer effect

It was found during the copolymerization reactions studied that styrene protects the TTC moiety from decomposition and depending on the amount in the initial composition, improves the reaction controlled character. The copolymerization reaction kinetics are discussed next.

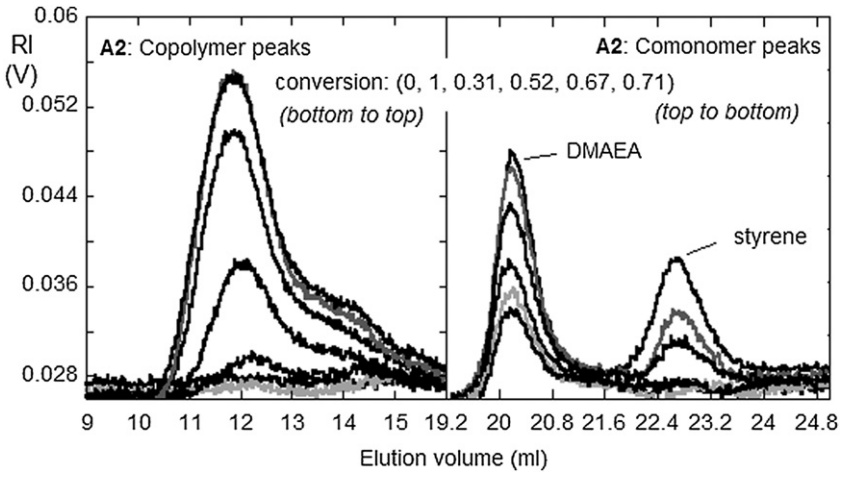

Fig. 9. SEC chromatograms containing RI copolymer and comonomer peaks vs. elution volume from samples taken during reaction A2 (DMAEA/Sty 95/5).

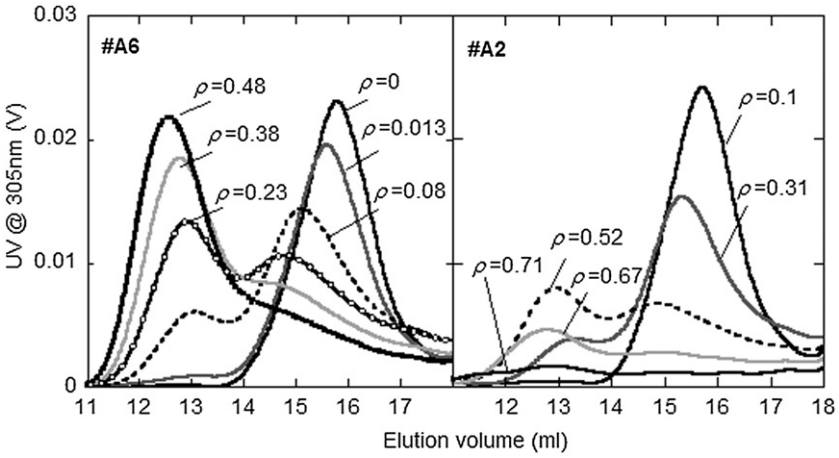

Fig. 10. SEC chromatograms containing UV absorbance @305 nm for samples withdrawn during reaction A2 (DMAEA/Sty (95/5)) and A6 (DMAEA/Sty (50/50)).

Continuous UV data at 305 nm provided by ACOMP, shown in Fig. 8, follow the evolution of the TTC during the copolymerization reactions listed in Table 1. The degradation process is slower for higher amount of styrene, also shown in the inset to figure where the TTC decomposition rate constants are plotted vs. styrene %. The decomposition rates were from exponential fits used as first-order approximations.

SEC experiments on samples taken during reactions confirm ACOMP findings and furnish additional evidence concerning TTC degradation and the loss of control by capturing the broadening in MWD for reactions with a high amount of DMAEA.

Thus, Fig. 9 shows RI chromatograms from SEC experiments on samples taken from the waste line during the reaction A2. The growing RI polymer peaks, following the increase in M_w, initially shift to the left as the reaction proceeds, as expected in CRP. However, the build up of a shoulder in the right side of the MWD indicates that termination occurs and leads to a significant percentage of dead chains, which leads eventually to loss of control. On the other hand, the well separated DMAEA and styrene RI peaks follow the consumption of the comonomers, and allow cross checks with ACOMP conversion, which are in excellent agreement.

For a better illustration of the effect of styrene on the TTC degradation, shown in Fig. 10 are SEC chromatograms for A2 and A6 experiments, containing UV at 305 nm, which monitors the depletion of the RAFT control agent, DoPAT, against incorporation of a TTC into the polymer chain. In the case of A6, a reaction with a high styrene%, the TTC changes from DoPAT to a macroRAFT and gradually converts into the final polymer, in a controlled fashion, indicated by the increase in the polymer peak and the shift toward lower elution volumes. Data for reaction A2, in stark contrast, show the formation of the macroRAFT followed by its decomposition, since it does not appear in the polymer peak. However, the corresponding RI SEC shown in Fig. 9 indicates that there actually is polymer formed.

Therefore, a possible explanation is that increasing the amount of styrene minimizes the side effects due to the interaction of the amine group in DMAEA with the trithiocarbonate group, by removing the TTC from the vicinity of the amine group. When the last monomer unit on the chain is DMAEA, the TTC is close to the amine and the two groups can react, but when the last monomer unit is styrene, the TTC is much further away from the amine and reaction is negligible. On the other hand, the relative leaving abilities of acrylyl and styryl radicals in the fragmentation step of a RAFT-controlled polymerization have to be considered. The acrylyl radical is a much better leaving group, and so will fragment off an intermediate RAFT radical much faster than a styryl radical will, with the result that the TTC will spend most of its time on styryl-ended polymer chains and thus be protected from reaction with the amine located one or more monomer units back along the chain. This rate difference should explain why degradation of the TTC seems to be completely stopped in the case of the reaction with 50% styrene.

Fig. 11 shows the way the incorporation of increasing styrene in the copolymer affects the evolution of the dispersity (M_w/M_n) and of the fraction of living chains (L) at same conversion for samples taken during reactions with different initial composition. The MWD narrowing with increasing styrene is further evidence that the styrene is protecting the RAFT control agent and fostering a living type polymerization.

The fraction of living chains (L) in each reaction was calculated based on the equation below [48].

$$L = \frac{(M_n - m_{DoPAT})[DoPAT]_0}{([M]_0 - [M]_t)m_M} \tag{9}$$

where m_M and m_{DoPAT} are the molecular mass of the monomer and of the RAFT control agent respectively, $[M]_0$ and $[DoPAT]_0$ are the

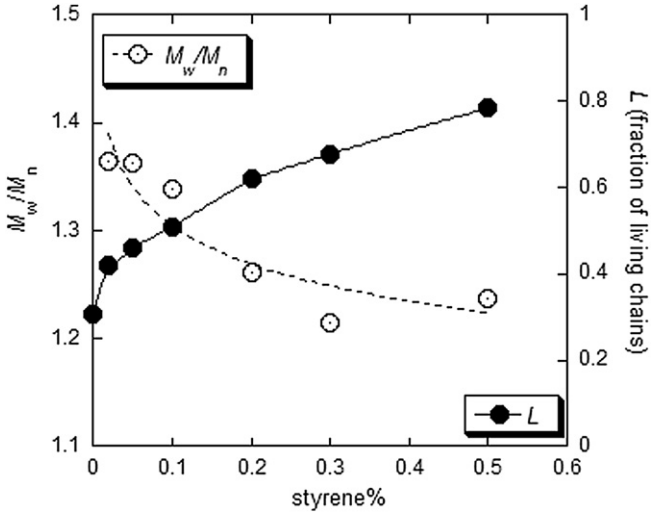

Fig. 11. M_w/M_n from SEC and fraction of the living chains, L from ACOMP as functions of the styrene % in the initial composition for reactions listed in Table 1.

initial concentrations of the monomer and of the RAFT control agent, $[M]_t$ is the concentration of the monomer at time t, M_n is calculated from SEC experiments.

The fraction of living chains clearly increases with the starting fraction of styrene, providing further evidence that styrene promotes the controlled behavior of the reaction.

4. Conclusions

Kinetics of copolymerization reactions of DMAEA and styrene in DMF and in the presence of trithiocarbonate RAFT control agents were followed by the use of the online monitoring method developed by the authors, ACOMP. Combined light scattering and spectroscopic measurements allowed conversion, copolymer mass, and gradient composition to be determined. The online monitoring allowed deviations from reaction control to be observed. It was found that the main CRP characteristics were compromised due to the decomposition of the controlling trithiocarbonate moiety in the presence of DMAEA. The presence of styrene in copolymer composition, led to better controlled reaction kinetics. The effect of different species on the degradation process was investigated. The continuous F_{inst} and M_w data provided by ACOMP allows assessment of the effect of the rate of styrene incorporation in the copolymer on the evolution of the reaction kinetics during the copolymerization.

Acknowledgments

The authors acknowledge support from NSF CBET 0623531, Louisiana Board of Regents ITRS RD-B-5, the Tulane Institute for Macromolecular Engineering and Science, and NASA NNX08AP04A. The authors gratefully thank Arkema Inc. and DuluxGroup Ltd. for donating the RAFT control agents.

Appendix A. Supplementary material

Supplementary data associated with this article can be found, in the online version, at doi:10.1016/j.polymer.2010.08.015

References

[1] Matyjaszewski K. Comparison and classification of controlled/living radical polymerizations. In: Matyjaszewski K, editor. Controlled/living radical polymerization. Progress in ATRP, NMP, and RAFT ACS symposium series, vol. 768. Washington: ACS; 2000. p. 2–26.
[2] Braunecker WA, Matyjaszewski K. Prog Polym Sci 2007;32:93–146.
[3] Kia J, Matyjaszewski K. Chem Rev 2001;101:2921–90.
[4] McCormick CL, Lowe AB. Acc Chem Res 2004;37:312–25.
[5] Moad G, Rizzardo E, Thang SH. Aust J Chem 2006;59:669–92.
[6] van den Dungen ETA, Rinquest J, Pretorius NO, McKenzie JM, McLeary JB, Sanderson RD, et al. Aust J Chem 2006;59:742–8.
[7] Patton D, Advincula R. Macromolecules 2006;39:8674–83.
[8] Puskas JE, Chan SWP, Kwon Y, McAuley KB, Shaikh S, Kaszas G. J Polym Sci Chem 2005;43:5394–413.
[9] Perrier S, Takolpuckdee P. J Polym Sci A Polym Chem 2005;43:5347–93.
[10] Mayadunne RTA, Rizzardo E. Mechanistic and practical aspects of RAFT polymerization. In: Jagur-Grodzinski J, editor. Living and controlled polymerization: synthesis, characterization and properties of the respective polymers and copolymers, vol. 65. New York: Nova Science Publishers; 2005.
[11] Moad G, Solomon DH. The chemistry of radical polymerization. 2nd ed. Oxford: Elsevier; 2006. p. 502.
[12] Lowe AB, McCormick CL. Prog Polym Sci 2007;32:283–351.
[13] Rizzardo E, Chen M, Chong B, Skidmore M, Thang SH. Macromol Symp 2007;248:104–16.
[14] Barner L, Davis TP, Stenzel M, Barner-Kowollik C. Macromol Rapid Commun 2007;28:539–59.
[15] Liu C, Hillmyer MA, Lodge TP. Langmuir 2009;5:13718–25.
[16] Smith AE, Xua X, McCormick CL. Prog Polym Sci 2010;35:45–93.
[17] Baussard J-F, Habib-Jiwanb J-L, Laschewskya A, Mertogluc M, Storsberg J. Polymer 2004;45:3615–26.
[18] Harisson S. Macromolecules 2009;42:897–8.
[19] Penczek S. J Polym Sci Part A Polym Chem 2002;40:1665–76.
[20] Florenzano FH, Strelitzki R, Reed WF. Macromolecules 1998;31:7226–38.
[21] Alb AM, Serelis AK, Reed WF. Macromolecules 2008;41:332–8.
[22] Alb AM, Drenski MF, Reed WF. Polym Int 2008;57:390–6.
[23] Feldermann A, Ah Toy A, Davis TP, Stenzel MH, Barner-Kowollik C. Polymer 2005;46:8448–57.
[24] Goto A, Sato K, Tsujii Y, Fukuda T, Moad G, Rizzardo E, et al. Macromolecules 2001;34:402–8.
[25] Theis A, Davis TP, Stenzel MH, Barner-Kowollik C. Polymer 2006;47:999–1010.
[26] Barner-Kowollik C, Buback M, Charleux B, Coote ML, Drache M, Fukuda T, et al. Polym Sci Part A Polym Chem 2006;44:5809–31.
[27] Coady DJ, Norris BC, Lynch VM, Bielawski CW. Macromolecules 2008;41:3775–8.
[28] Alb AM, Drenski MF, Reed WF. J Appl Polym Sci 2009;113:190–8.
[29] Zetterlund PB, Kagawa Y, Okubo M. Chem Rev 2008;108:3747–94.
[30] Alexandridis P, Lindman B, editors. Amphiphilic block copolymers: self-assembly and applications. Amsterdam: Elsevier Science; 2000.
[31] Suchao-in N, Chirachanchai S, Perrier S. Polymer 2009;50:4151–8.
[32] Morgan SE, Jones P, Lamont AS, Heidenreich A, McCormick CL. Langmuir 2007;23:230–40.
[33] Rowe MD, Chang C-C, Thamm DH, Kraft SL, Harmon JF, Vogt AP, et al. Langmuir 2009;25:9487–99.
[34] Zeng F, Shen Y, Zhu S. Macromol Rapid Commun 2002;23:1113–7.
[35] Convertine AJ, Benoit DSW, Duvall CL, Hoffman AS, Stayton PS. Controlled Release 2009;133:221–9.
[36] Ferguson CJ, Hughes RJ, Nguyen D, Pham BTT, Gilbert RG, Serelis AK, et al. Macromolecules 2005;38:2191–204.
[37] Mayadunne RTA, Rizzardo E, Chiefari J, Krstina J, Moad G, Postma A, et al. Macromolecules 2000;33:243–5.
[38] Alb AM, Reed WF. Macromolecules 2008;41:2406–14.
[39] Norwood DP, Reed WF. Int J Pol Anal Charact 1997;4:99–132.
[40] Enohnyaket P, Kreft T, Alb AM, Drenski MF, Reed WF. Macromolecules 2007;40:8040–9.
[41] Kreft T, Reed WF. J Phys Chem B 2009;113:8303–9.
[42] Mignard E, Leblanc T, Bertin D, Guerret O, Reed WF. Macromolecules 2004;37:966–75.
[43] Zimm BH. J Chem Phys 1948;16:1093–100.
[44] Bian K, Cunningham MF. J Polym Sci Part A Polym Chem 2006;44:414–26.
[45] Sun X, Luo Y, Wang R, Li B-G, Liu B, Zhu S. Macromolecules 2007;40:849–59.
[46] Saikia PJ, Lee JM, Lee K, Choe S. J Polym Sci Part A Polym Chem 2008;46:872–85.
[47] Feldermann A, Stenzel MH, Davis TP, Vana P, Barner-Kowollik C. Macromolecules 2004;37:2404–10.
[48] Netopilik M, Kratochvil P. Polymer 2003;44:3431–6.
[49] Guillaneuf Y, Castignolles P. J Polym Sci Part A Polym Chem 2008;46:897–911.
[50] Gruendling T, Pickford R, Guilhaus M, Barner-Kowollik C. J Polym Sci Part A Polym Chem 2008;46:7447–61.